

Design, Synthesis and Biological Evaluation of Pazopanib Derivatives as Antitumor Agents

Yuping Jia^{1,†}, Jian Zhang^{2,†}, Jinhong Feng³,
Fuming Xu², Huili Pan² and Wenfang Xu^{2,*}

¹Shandong Institute of Pharmaceutical Industry, Ji'nan, Shandong 250101, China

²Department of Medicinal Chemistry, School of Pharmaceutical Sciences, Shandong University, Ji'nan, Shandong 250012, China

³Shandong Analysis and Test Center, Shandong Academy of Sciences, Ji'nan, Shandong 250012, China

*Corresponding author: Wenfang Xu, xuwenf@sdu.edu.cn

[†]These authors contributed equally to this work.

A novel series of pazopanib derivatives were designed, synthesized, and evaluated for their inhibitory activity against a series of kinases including VEGFR-2, EGFR, AKT1, ALK1, and ABL1. The anti-angiogenic activities *ex vivo* of some compounds were also investigated. Compounds P2d and P2e demonstrated outstanding inhibitory activity against VEGFR-2 and ABL1 and higher anti-angiogenic activity compared with Pazopanib, the reference standard. These two compounds (P2d and P2e) could be used as novel lead compounds for further development of anticancer agents.

Key words: anti-angiogenesis, antitumor agent, pazopanib derivatives, synthesis

Received 2 July 2013, revised 22 September 2013 and accepted for publication 27 September 2013

Tumor angiogenesis is a prerequisite for tumor cell proliferation, invasion, and metastasis. The formation of newly tumor-induced vessels can not only contribute to nutrient supply and metabolic waste removal for the tumor tissues but also facilitate metastasis formation for solid tumors (1–3). Protein kinases, especially by protein tyrosine kinases (PTKs) including epidermal growth factor receptor (EGFR) and vascular endothelial growth factor receptors (VEGFRs), play a pivotal role in signal transduction pathways tightly associating with angiogenesis (4,5). Therefore, the inhibition of angiogenesis is one of the effective methods for the treatment of cancer and design of small molecule angiogenesis inhibitors which has attracted great attention.

So far, many small molecule angiogenesis inhibitors have been synthesized and approved to be potent anticancer agents, exemplified by VEGF/VEGFR inhibitors (6,7).

Among them, Pazopanib, showed good potency against c-Kit (IC_{50} = 74 nM), PDGFR (IC_{50} = 84 nM), and VEGFR-1, -2, -3 (IC_{50} = 10, 30, and 47 nM, respectively) (8,9). Pazopanib was also approved to be an efficient drug for clinical treatment of advanced renal cell carcinoma (RCC) in 2009 (10,11). Due to the advantage of broad-spectrum anticancer potency and well tolerated results in clinical trials (12,13), the optimization of pazopanib is currently of great interest.

Based on the binding mode of pazopanib with VEGFR-2, indazole part projects into the back lipophilic pocket of VEGFR-2, and the pyrimidine N-1 and the C-2 anilino N-H bind ATP site with hydrogen bonds (9). This study is focused on the synthesis of new pazopanib derivatives bearing the same indazole and pyrimidine moieties as pazopanib and differing from the parent drug in the aniline or benzylamine part (Figure 1) which may improve the binding ability of the compound with the lipophilic residues of enzyme. For example, the sulfonamide is removed from the ortho-position to the para-position, and some derivatizations were also carried out on the sulfonamide moiety. To compare with benzenesulfonamide series, we also prepared some benzylamine derivatives without sulfonamido substituents. In addition, substitution at the amino nitrogen at C-6 indazole was also considered. The preliminary biological activity of all the target compounds against VEGFR-2, EGFR, AKT1, ALK1 and ABL1 were evaluated, and the anti-angiogenesis activities *ex vivo* of some compounds were also investigated. Furthermore, some structure activity relationships have also been established.

Methods and Materials

Chemistry

All the materials were purchased from commercial vendors and used without further purification unless otherwise specified. Solvents were dried over $CaCl_2$ or distilled prior to use and flash chromatography was performed using silica gel (200–300 mesh). All reactions were monitored by thin layer chromatography on 0.25 mm silica gel plates (60GF-254) and visualized with UV light. Proton NMR spectra were determined on a Bruker DRX 600/300 spectrometer using TMS as an internal standard in $DMSO-d_6$ or $CDCl_3$ solutions. ESI-MS were determined on an API 4000 spectrometer. Melting points were

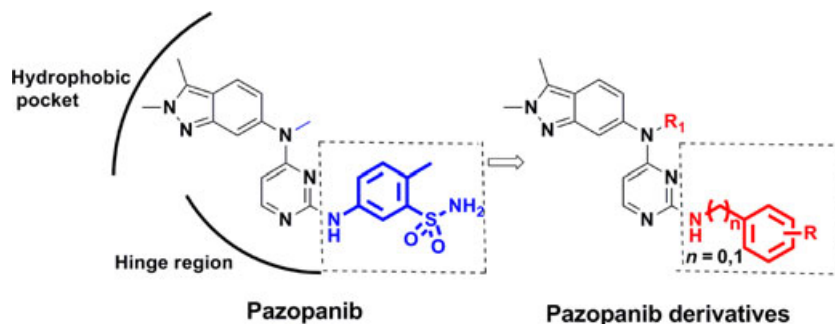
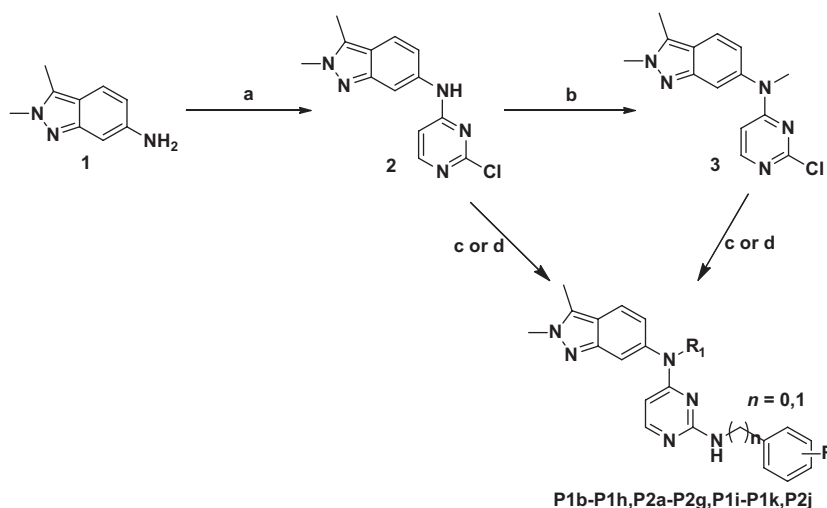


Figure 1: Structures of pazopanib and pazopanib derivatives.



Scheme 1: Reagents and Conditions: (a) 2, 4-dichloropyrimidine, NaHCO_3 , THF/EtOH, 75 °C (b) iodomethane, Cs_2CO_3 , DMF, rt (c) conc. HCl, isopropanol, 85 °C (d) Cs_2CO_3 , dioxane, 105 °C.

conducted on electrothermal melting point apparatus (uncorrected). The synthetic route was shown in Scheme 1.

Preparation of N-(2-chloropyrimidin-4-yl)-2,3-dimethyl-2H-indazole-6-amine (compound 2)

To a stirred solution of **1** (0.18 g, 1 mmol) and NaHCO_3 (0.34 g, 4 mmol) in THF (2 mL) and EtOH (8 mL) was added 2, 4-dichloropyrimidine (0.45 g, 3 mmol) at room temperature. The reaction was stirred at 75 °C overnight, and the resulting suspension was filtered and the filtrate was concentrated under vacuum to leave residue. The residue was washed thoroughly with Et_2O to remove excess 2,4-dichloropyrimidine to afford compound **2** (0.26 g, 95.2% yield). mp: 215–216 °C, ESI-MS m/z : 274.2 $[\text{M} + \text{H}]^+$; $^1\text{H-NMR}$ (600 MHz, $\text{DMSO}-d_6$): δ 10.00 (s, 1H), 8.13 (d, $J = 6.0$ Hz, 1H), 7.63 (d, $J = 9.0$ Hz, 1H), 6.98 (d, $J = 8.4$ Hz, 1H), 6.77 (d, $J = 6.0$ Hz, 1H), 4.01 (s, 3H), 2.54 (s, 3H).

Preparation of N-(2-chloropyrimidin-4-yl)-N, 2, 3-trimethyl-2H-indazole-6-amine (compound 3)

Cs_2CO_3 (0.276 g, 2 mmol) was added portionwise to a solution of **2** (0.27 g, 1 mmol) in DMF (10 mL) and the reaction solution stirred at room temperature for 10 min.

Iodomethane (0.1 mL, 1.5 mmol) was then added and the mixture was stirred for 24 h. The reaction mixture was then diluted with water (50 mL) and extracted with EtOAc (3 \times 50 mL). The organic layer was dried over MgSO_4 , filtered, and evaporated to yield a crude product that was subjected to silica gel chromatography eluting with $\text{CH}_2\text{Cl}_2/\text{MeOH}$ (60:1 v/v) to give compound **3** (0.09 g, 31% yield). mp: 172–173 °C, ESI-MS m/z : 288.2 $[\text{M} + \text{H}]^+$; $^1\text{H-NMR}$ (600 MHz, $\text{DMSO}-d_6$): δ 7.95 (s, $J = 6.0$ Hz, 1H), 7.80 (d, $J = 9.0$ Hz, 1H), 7.51 (s, 1H), 6.88 (d, $J = 9.0$ Hz, 1H), 6.24 (d, $J = 6.0$ Hz, 1H), 4.05 (s, 3H), 3.31 (s, 3H), 2.51 (s, 3H).

Preparation of pazopanib

To a solution of compound **3** (0.20 g, 0.695 mmol) and 5-amino-2-methylbenzenesulfonamide (0.13 g, 0.695 mmol) in IPA (6 mL) was added 4 drops of Conc. HCl, and the mixture was heated to reflux with stirring overnight. The mixture was allowed to cool to room temperature and the resulting precipitate was collected via filtration and washed with Et_2O to yield Pazopanib (0.3 g, 90% yield). mp: 236–237 °C, ESI-MS m/z : 438.5 $[\text{M} + \text{H}]^+$; $^1\text{H-NMR}$ (600 MHz, $\text{DMSO}-d_6$): δ 10.39 (s, 1H), 8.60 (s, 1H), 7.82 (d, $J = 6.0$ Hz, 1H), 7.76 (d, $J = 8.4$ Hz, 1H), 7.72 (d, $J = 8.8$ Hz, 1H), 7.44 (s, 1H), 7.16 (s, 1H), 7.12 (s, 2H), 5.86 (s, 1H), 6.88 (d, $J = 7.2$ Hz, 1H), 4.04 (s, 3H), 3.42

(s, 3H), 3.32 (s, 3H), 2.55 (s, 3H). HRMS (AP-ESI) m/z : calcd for $C_{21}H_{23}N_7O_2S$ $[M + H]^+$ 438.1707, found 438.1708.

The compounds **P1b-P1h** and **P2a-P2g** were synthesized following the general procedure as described above (preparation of Pazopanib).

4-((4-((2,3-dimethyl-2H-indazole-6-yl)amino)pyrimidin-2-yl)amino)benzenesulfonamide (P1b)

A white solid, yield: 88%, mp: 239–240 °C, ESI-MS m/z : 410.5 $[M + H]^+$; 1H -NMR (600 MHz, DMSO- d_6): δ 10.25 (s, 1H), 10.18 (s, 1H), 8.06 (d, J = 6.3 Hz, 1H), 7.97 (s, 1H), 7.89 (d, J = 8.7 Hz, 2H), 7.72 (d, J = 8.7 Hz, 2H), 7.64 (d, 1H), 7.25 (s, 2H), 7.09 (d, 1H), 6.45 (d, 1H), 4.04 (s, 3H), 2.60 (s, 3H).

4-((4-((2,3-dimethyl-2H-indazole-6-yl)amino)pyrimidin-2-yl)amino)-N-(pyrimidin-2-yl)benzenesulfonamide (P1c)

A white solid, yield: 92%, mp: 206–208 °C, ESI-MS m/z : 488.5 $[M + H]^+$; 1H -NMR (300 MHz, DMSO- d_6): δ 11.23 (s, 1H), 10.19 (s, 1H), 8.48 (d, J = 4.8 Hz, 2H), 8.07 (d, J = 6.9 Hz, 1H), 7.68–7.91 (m, 6H), 7.12 (d, J = 8.7 Hz, 1H), 7.04 (t, 1H), 6.61 (d, J = 7.2 Hz, 1H), 4.09 (s, 3H), 2.64 (s, 3H).

4-((4-((2,3-dimethyl-2H-indazole-6-yl)amino)pyrimidin-2-yl)amino)-N-(4-methylpyrimidin-2-yl)benzenesulfonamide (P1d)

A white solid, yield: 96%, mp: 212–214 °C, ESI-MS m/z : 502.5 $[M + H]^+$; 1H -NMR (300 MHz, DMSO- d_6): δ 11.47 (s, 1H), 11.37 (s, 1H), 8.29 (d, J = 5.1 Hz, 1H), 8.09 (d, J = 7.2 Hz, 1H), 7.91 (d, J = 8.7 Hz, 2H), 7.84 (s, 1H), 7.67–7.78 (m, 4H), 7.21 (d, J = 8.7 Hz, 1H), 6.89 (d, J = 5.1 Hz, 1H), 6.67 (d, J = 6.9 Hz, 1H), 4.11 (s, 3H), 2.66 (s, 3H), 2.25 (s, 6H).

4-((4-((2,3-dimethyl-2H-indazole-6-yl)amino)pyrimidin-2-yl)amino)-N-(4,6-dimethylpyrimidin-2-yl)benzenesulfonamide (P1e)

A white solid, yield: 86%, mp: 224–225 °C, ESI-MS m/z : 516.6 $[M + H]^+$; 1H -NMR (300 MHz, DMSO- d_6): δ 11.09 (s, 1H), 11.04 (s, 1H), 8.05 (d, J = 7.2 Hz, 1H), 7.90 (d, J = 8.7 Hz, 2H), 7.83 (s, 1H), 7.69–7.76 (m, 4H), 7.11 (d, J = 8.7 Hz, 1H), 6.74 (s, 1H), 6.56 (d, J = 7.2 Hz, 1H), 4.08 (s, 3H), 2.64 (s, 3H), 2.19 (s, 6H).

4-((4-((2,3-dimethyl-2H-indazole-6-yl)amino)pyrimidin-2-yl)amino)-N-(5-methylisoxazol-3-yl)benzenesulfonamide (P1f)

A white solid, yield: 92%, mp: 216–217 °C, ESI-MS m/z : 491.5 $[M + H]^+$; 1H -NMR (300 MHz, DMSO- d_6): δ 11.44

(s, 1H), 11.22 (s, 1H), 8.07 (d, J = 6.9 Hz, 1H), 7.86 (s, 1H), 7.80 (m, 4H), 7.72 (d, J = 9.0 Hz, 1H), 7.14 (d, J = 9.0 Hz, 1H), 6.61 (d, J = 7.2 Hz, 1H), 6.13 (d, J = 9.0 Hz, 1H), 4.08 (s, 3H), 2.65 (s, 3H), 2.24 (s, 3H).

N-carbamimidoyl-4-((4-((2,3-dimethyl-2H-indazole-6-yl)amino)pyrimidin-2-yl)amino)benzenesulfonamide (P1g)

A white solid, yield: 90%, mp: 182–183 °C, ESI-MS m/z : 452.5 $[M + H]^+$; 1H -NMR (300 MHz, DMSO- d_6): δ 11.45 (s, 1H), 11.21 (s, 1H), 8.07 (d, J = 7.2 Hz, 1H), 7.89 (s, 1H), 7.66–7.99 (m, 5H), 7.26 (d, J = 8.4 Hz, 1H), 6.94 (s, 4H), 6.67 (d, J = 6.6 Hz, 1H), 4.09 (s, 3H), 2.65 (s, 3H).

N⁴-(2,3-dimethyl-2H-indazole-6-yl)-N²-(4-fluorophenyl)pyrimidine-2,4-diamine (P1h)

A white solid, yield: 95%, mp: 219–220 °C, ESI-MS m/z : 349.4 $[M + H]^+$; 1H -NMR (300 MHz, DMSO- d_6): δ 11.06 (s, 1H), 10.76 (s, 1H), 7.97 (d, J = 7.2 Hz, 1H), 7.90 (s, 1H), 7.69 (d, J = 7.5 Hz, 1H), 7.56–7.60 (m, 2H), 7.23 (d, 2H), 7.14 (d, J = 8.7 Hz, 1H), 6.55 (d, J = 6.9 Hz, 1H), 4.04 (s, 3H), 2.61 (s, 3H).

4-((4-((2,3-dimethyl-2H-indazole-6-yl)(methyl)amino)pyrimidin-2-yl)amino)benzenesulfonamide (P2b)

A white solid, yield: 89%, mp: >270 °C, ESI-MS m/z : 424.5 $[M + H]^+$; 1H -NMR (300 MHz, DMSO- d_6): δ 10.20 (s, 1H), 7.92 (d, J = 6.6 Hz, 1H), 7.82 (d, J = 9.0 Hz, 1H), 7.79 (s, 1H), 7.76 (s, 1H), 7.63 (d, J = 6.9 Hz, 1H), 7.563 (s, 1H), 7.22 (s, 2H), 6.92 (d, J = 9.0 Hz, 1H), 4.08 (s, 3H), 3.53 (s, 3H), 2.65 (s, 3H).

4-((4-((2,3-dimethyl-2H-indazole-6-yl)(methyl)amino)pyrimidin-2-yl)amino)-N-(pyrimidin-2-yl)benzenesulfonamide (P2c)

A white solid, yield: 84%, mp: 244–245 °C, ESI-MS m/z : 502.4 $[M + H]^+$; 1H -NMR (300 MHz, DMSO- d_6): δ 11.08 (s, 1H), 8.50 (d, J = 4.8 Hz, 2H), 7.97 (s, 1H), 7.88 (d, J = 9.0 Hz, 1H), 7.60–7.73 (m, 4H), 7.06 (t, 1H), 6.94 (d, J = 8.7 Hz, 1H), 6.12 (s, 1H), 4.09 (s, 3H), 3.57 (s, 3H), 2.64 (s, 3H). HRMS (AP-ESI) m/z : calcd for $C_{24}H_{23}N_9O_2S$ $[M + H]^+$ 502.1768, found 502.1768.

4-((4-((2,3-dimethyl-2H-indazole-6-yl)(methyl)amino)pyrimidin-2-yl)amino)-N-(4-methylpyrimidin-2-yl)benzenesulfonamide (P2d)

A white solid, yield: 80%, mp: >270 °C, ESI-MS m/z : 516.6 $[M + H]^+$; 1H -NMR (300 MHz, DMSO- d_6): δ 10.75 (s, 1H), 8.31 (d, J = 5.4 Hz, 1H), 7.94 (d, J = 7.2 Hz, 1H), 7.86 (d, J = 8.7 Hz, 1H), 7.58–7.71 (m, 4H), 6.92 (d, J = 8.7 Hz, 2H), 6.14 (s, 1H), 4.10 (s, 3H), 3.56 (s, 3H),

3.67 (s, 3H), 2.31 (s, 3H). HRMS (AP-ESI) *m/z*: calcd for C₂₅H₂₅N₉O₂S [M + H]⁺ 516.1925, found 516.1926.

4-((4-((2,3-dimethyl-2H-indazole-6-yl)(methyl)amino)pyrimidin-2-yl)amino)-N-(4,6-dimethylpyrimidin-2-yl)benzenesulfonamide (P2e)

A white solid, yield: 90%, mp: 226–228 °C, ESI-MS *m/z*: 530.3 [M + H]⁺; ¹H-NMR (300 MHz, DMSO-*d*₆): δ 11.50 (s, 1H), 11.04 (s, 1H), 7.92 (d, *J* = 6.6 Hz, 1H), 7.77–7.81 (m, 4H), 7.50 (s, 1H), 6.90 (d, *J* = 6.9 Hz, 1H), 6.76 (s, 1H), 5.98 (d, *J* = 6.0 Hz, 1H), 4.08 (s, 3H), 3.50 (s, 3H), 2.65 (s, 3H), 2.25 (s, 6H). HRMS (AP-ESI) *m/z*: calcd for C₂₆H₂₇N₉O₂S [M + H]⁺ 530.2081, found 530.2082.

4-((4-((2,3-dimethyl-2H-indazole-6-yl)(methyl)amino)pyrimidin-2-yl)amino)-N-(5-methylisoxazol-3-yl)benzenesulfonamide (P2f)

A white solid, yield: 87%, mp: 230–231 °C, ESI-MS *m/z*: 505.3 [M + H]⁺; ¹H-NMR (300 MHz, DMSO-*d*₆): δ 11.32 (s, 1H), 10.62 (s, 1H), 7.95 (d, *J* = 6.9 Hz, 1H), 7.85 (s, 1H), 7.64–7.82 (m, 4H), 7.55 (s, 1H), 6.11 (s, 1H), 6.07 (s, 1H), 4.09 (s, 3H), 3.55 (s, 3H), 2.66 (s, 3H), 2.31 (s, 3H). HRMS (AP-ESI) *m/z*: calcd for C₂₄H₂₄N₈O₃S [M + H]⁺ 505.1765, found 505.1765.

N-carbamimidoyl-4-((4-((2,3-dimethyl-2H-indazole-6-yl)(methyl)amino)pyrimidin-2-yl)amino)benzenesulfonamide (P2g)

A white solid, yield: 86%, mp: 244–246 °C, ESI-MS *m/z*: 466.5 [M + H]⁺; ¹H-NMR (300 MHz, DMSO-*d*₆): δ 11.13 (s, 1H), 11.01 (s, 1H), 8.03 (d, *J* = 7.2 Hz, 1H), 7.90 (s, 1H), 7.70–7.72 (m, 5H), 7.13 (d, *J* = 8.4 Hz, 1H), 6.78 (s, 4H), 6.57 (d, *J* = 6.9 Hz, 1H), 4.07 (s, 3H), 2.63 (s, 3H).

Preparation of N²-benzyl-N⁴-(2,3-dimethyl-2H-indazole-6-yl)pyrimidine-2, 4-diamine (P1i)

To a solution of compound **2** (0.082 g, 0.3 mmol) and Cs₂CO₃ (0.14 g, 1 mmol) in dioxane (10 mL) was added dropwise of benzylamine, and the mixture was heated at 105 °C overnight. The mixture was allowed to cool to room temperature, filtered, and evaporated to yield a crude product that was subjected to silica gel chromatography eluting with CH₂Cl₂/MeOH (60:1 v/v) to give compound **P1i** (0.052 g, 50% yield). mp: 131–132 °C, ESI-MS *m/z*: 345.4 [M + H]⁺; ¹H-NMR (300 MHz, DMSO-*d*₆): δ 10.59 (s, 1H), 8.63 (s, 1H), 8.02 (s, 1H), 7.85 (d, *J* = 6.9 Hz, 1H), 7.60 (d, *J* = 9.0 Hz, 1H), 7.23–7.41 (m, 5H), 7.06 (d, 1H), 6.32 (s, 1H), 4.59 (d, *J* = 5.4 Hz, 2H), 4.02 (s, 3H), 2.58 (s, 3H).

The compounds **P1j–P1k** and **P2j** were synthesized following the general procedure as described above (preparation of **P1i**).

N⁴-(2,3-dimethyl-2H-indazole-6-yl)-N²-(4-fluorobenzyl)pyrimidine-2,4-diamine (P1j)

A white solid, yield: 42%, mp: 198–200 °C, ESI-MS *m/z*: 363.4 [M + H]⁺; ¹H-NMR (300 MHz, DMSO-*d*₆): δ 9.84 (s, 1H), 8.10 (s, 1H), 7.84 (d, *J* = 6.3 Hz, 1H), 7.55 (d, *J* = 8.7 Hz, 1H), 7.42 (m, 2H), 7.15 (m, 2H), 6.01 (s, *J* = 9.0 Hz, 1H), 6.15 (d, *J* = 6.0 Hz, 2H), 4.51 (d, *J* = 6.0 Hz, 2H), 4.00 (s, 3H), 2.56 (s, 3H).

N⁴-(2,3-dimethyl-2H-indazole-6-yl)-N²-(4-methoxybenzyl)pyrimidine-2,4-diamine (P1k)

A white solid, yield: 48%, mp: 195–196 °C, ESI-MS *m/z*: 375.5 [M + H]⁺; ¹H-NMR (600 MHz, DMSO-*d*₆): δ 9.09 (s, 1H), 8.19 (s, 1H), 7.82 (d, *J* = 6.0 Hz, 1H), 7.50 (d, *J* = 8.4 Hz, 1H), 7.28–7.51 (m, 4H), 7.28 (s, 1H), 6.98 (d, *J* = 9.6 Hz, 1H), 6.02 (d, 1H), 4.43 (d, 2H), 3.98 (s, 3H), 3.71 (s, 3H), 2.50 (s, 3H).

N⁴-(2,3-dimethyl-2H-indazole-6-yl)-N²-(4-fluorobenzyl)-N⁴-methylpyrimidine-2,4-diamine (P2j)

A white solid, yield: 39%, mp: 219–220 °C, ESI-MS *m/z*: 377.5 [M + H]⁺; ¹H-NMR (300 MHz, DMSO-*d*₆): δ 8.60 (s, 1H), 7.82 (s, *J* = 8.7 Hz, 1H), 7.70 (d, *J* = 7.2 Hz, 1H), 7.54 (s, 1H), 7.37–7.42 (m, 2H), 7.14–7.20 (m, 2H), 6.90 (d, *J* = 8.7 Hz, 1H), 5.77 (d, *J* = 6.6 Hz, 1H), 4.55 (d, *J* = 5.7 Hz, 2H), 4.07 (s, 3H), 3.48 (s, 3H), 2.63 (s, 3H).

In vitro kinase inhibition assay

IC₅₀ values against kinases were determined using the Z-lyte™ biochemical assay which employed a FRET-based, coupled-enzyme format and was based on the differential sensitivity of phosphorylated and non-phosphorylated peptides to proteolytic cleavage. The kinase inhibitory activity of compounds was profiled by screening: 2.5 μL of different concentrate of the test compounds, Pazopanib or water (control) were added to the kit and incubated for 1 h at room temperature followed by the addition of 5 μL development reagent A. One h later, the reaction was stopped by adding 5 μL stop reagent. The fluorescence intensity at 445 and 520 nm were monitored through an EnVision multilabel plate reader. The standard inhibitory reference compound was Staurosporine. The experiment was performed in duplicate.

Rat thoracic aorta rings (TARs) assay

The artery was isolated from 8 to 10-week-old male Sprague Dawley rats (250 g) and was washed in PBS. After careful removal of fibroadipose tissues, it was cut into 1-mm-thick aortic rings and embedded in BD Matrigel (BD Biosciences, San Jose, CA, USA) in a 96-well plate. The rings were incubated at 37 °C and 5% CO₂ for half an hour and 100 μL of different concentrate of inhibitors in medium was added. Aortic rings were treated every

Table 1: Structures of target compounds and their inhibition to ABL1, AKT1, ALK1, EGFR and VEGFR-2

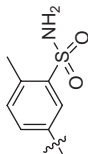
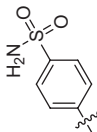
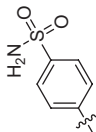
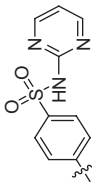
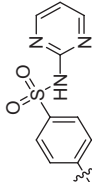
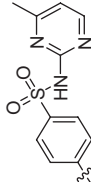
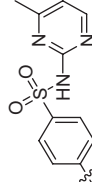
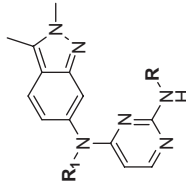
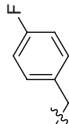
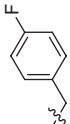
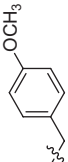
Compound	Structure R	Inhibition rates ^a (%)						
		R ₁	ABL1	AKT1	ALK1	EGFR	VEGFR-2	
Pazopanib		CH ₃	92.26	3.13	93.68	79.40	100.32	
P1b		H	31.10	3.76	4.26	20.66	60.81	
P2b		CH ₃	93.50	3.60	84.91	55.81	97.48	
P1c		H	93.06	3.97	96.85	41.68	98.53	
P2c		CH ₃	100.34	2.74	61.89	27.59	100.56	
P1d		H	96.22	2.35	100.68	31.60	94.58	
P2d		CH ₃	100.19	3.56	32.99	35.87	99.74	

Table 1: continued

Compound	Structure R	Inhibition rates ^a (%)					
		R ₁	ABL1	AKT1	ALK1	EGFR	VEGFR-2
P1e		H	98.55	1.90	84.88	48.40	99.25
P2e		CH ₃	94.93	-0.14	11.79	20.67	100.12
P1f		H	82.43	56.02	64.80	29.05	92.43
P2f		CH ₃	97.96	8.48	53.41	46.83	98.62
P1g		H	91.87	1.21	82.78	69.41	95.73
P2g		CH ₃	94.12	28.24	64.90	75.58	94.28
P1h		H	75.02	2.10	37.57	55.80	63.82

Table 1: continued

Compound	Structure R	Inhibition rates ^a (%)						
		R ₁	ABL1	AKT1	ALK1	EGFR	VEGFR-2	
P1i		H	17.39	5.41	23.77	42.09	ND	
P1j		H	8.68	1.28	12.92	26.28	32.68	
P2j		CH ₃	14.56	4.00	0.84	26.41	37.54	
P1k		H	5.96	0.78	25.07	19.90	ND	

ND, Not determined.

^aThe percent inhibition was measured for each compound at the concentration of 10 μM.

other day with either RPMI1640 medium, Pazopanib, or synthesized compounds for 6 days and photographed on the 7th day at $\times 4$ magnification. Experiments were repeated three times using artery from three different male rats.

Results and Discussion

Synthesis

The target compounds were synthesized efficiently as outlined in Scheme 1. The intermediate **2** was prepared from 2, 3-dimethyl-6-amino-2*H*-indazole **1**, which was treated with excess 2, 4-dichloropyrimidine to generate substituted compound **2**. Then methyl intermediate **3** was obtained by treating **2** with iodomethane, and was treated with corresponding amine (substituted aniline and benzylamine) to generate target compounds **P1b-P1h**, **P2b-P2g** and target compounds **P1i-P1k**, **P2j**. All the title compounds were confirmed by ^1H NMR and MS.

In vitro protein kinase assay

As the member of the receptor tyrosine kinase family, VEGFRs and EGFRs are the most important receptors for angiogenesis, which can initiate PI3K/AKT signaling pathways that stimulate angiogenesis (5,14). Activation of the EGFR pathway increased the production of tumor-derived VEGF that acted on endothelial cells in a paracrine manner to promote angiogenesis (15). ALK1 which was required for angiogenesis was an orphan type I receptor of the TGF- β 1 receptor family (16). TGF- β 1 is an extremely potent stimulator for the production of VEGF (17). ABL1 is a ubiquitously expressed non-receptor tyrosine kinase implicated in the regulation of cell proliferation, survival, and migration (18).

To know about effects of compounds on these kinases, the preliminary kinase assay of ABL1, AKT1, ALK1, EGFR, and VEGFR-2 *in vitro* was carried out to evaluate the potential inhibitory activities of the target compounds at the concentration of 10 μM . As shown in Table 1, most compounds possessed potent inhibitory activities towards VEGFR-2, ABL1, and ALK1 and moderate inhibitory activity towards EGFR. In contrast, few compounds showed inhibitory activity against AKT1 that is a serine/threonine kinase, which might indicate some relative selectivity of these compounds towards tyrosine kinase, which needed further investigation.

According to the data listed in Table 1, compounds **P1c-g** and **P2b-g**, of which the percent inhibition were higher than 80, were chosen to test the IC_{50} values of ABL1, VEGFR-2, and EGFR (Table 2), and most of them (except **P2b**, **P1f** and **P1g**) exhibited comparable inhibitory activity to Pazopanib against ABL1. Notably, compounds **P2d**, **P2e** (IC_{50} = 0.062 μM and 0.022 μM , respectively) demonstrated more potent inhibitory activity compared with

Table 2: The IC_{50} values against kinases of some compounds

Compound	IC_{50}^a (μM)		
	VEGFR-2	ABL1	EGFR
Pazopanib	0.043	0.62	5.95
P2b	0.87	1.35	ND ^b
P1c	0.034	0.46	ND ^b
P2c	0.029	0.12	ND ^b
P1d	0.16	0.28	ND ^b
P2d	0.025	0.062	ND ^b
P1e	0.12	0.36	ND ^b
P2e	0.012	0.022	ND ^b
P1f	1.63	2.18	ND ^b
P2f	0.65	0.32	ND ^b
P1g	1.34	0.93	ND ^b
P2g	0.72	0.36	1.37

^aValues are means of three experiments.

^bND, not determined because of low inhibition rates at 10 μM .

Pazopanib (IC_{50} = 0.62 μM). For VEGFR-2 inhibition assay, compounds **P2d** (IC_{50} = 0.025 μM) and **P2e** (IC_{50} = 0.012 μM) showed comparable inhibitory activity against VEGFR-2 compared with Pazopanib (IC_{50} = 0.043 μM).

The basic structure-activity relationship (SAR) were also studied: (i) Most benzenesulfonamido derivatives (**P1c-g** and **P2b-g**) displayed potent enzymic inhibitory activity against VEGFR-2, ABL1, ALK, whereas the benzylamine-substituted ones (**P1h-k** and **P2j**) showed less enzymic inhibitory activity, which indicated the importance of sulfonamide on the enzymic inhibitory activity. (ii) Among the benzenesulfonamide series, the compounds (**P1c**, **P2c**, **P1d**, **P2d**, **P1e**, and **P2e**) containing the pyrimidine structure on the sulfonamide moiety generally showed more potent enzymatic inhibitory activity when compared with other compounds without derivatizing the sulfonamide moiety. (iii) The methyl-substituted or unsubstituted of 4-amino made no great difference to the inhibitory activity, but the methyl-substituted ones showed a little better activity.

Rat thoracic aorta rings (TARs) assay

TARs assay which was more close to *in vivo* condition of angiogenesis was conducted to evaluate the anti-angiogenic effect of these Pazopanib derivatives. The results are shown in Tables 3 and 4, Figures 2 and 3. In control group, the sprouting endothelial cells began to migrate into the matrix and form capillary network of microvascular outgrowth at the luminal cut edges of the aortic fragments on day 3 (Figure 2A); the number of microvascular outgrowth was observed on day 7 (Figure 2B). In drug groups, compounds **P2b**, **P1c**, **P2c**, **P1d**, **P1e**, **P1f**, **P1g**, and **P1h** exhibited the similar anti-angiogenic activity when compared with pazopanib (Table 4). Especially, compounds **P2d**, **P2e** showed excellent anti-angiogenic activity than that of pazopanib and even could reduce microvascular

Table 3: The meaning on the tube formation

Picture				
Meaning	—	±	+	++
—: Means no cells growth. ±: Means several cells growth, but no tube formation. +: Means the sprouting endothelial cells began to form acapillary network. ++: Means a lot of capillary network were observed.				

Table 4: Effect of series 1 compounds on the tube formation

Compound	P2b	P1c	P2c	P1d	P2d	P1e	P2e	P1f	P2f	P1g	P2g	P1h	Pazopanib
0.1 μM	—	—	—	—	—	—	—	—	+	—	+	—	—
0.01 μM	±	±	+	±	—	+	—	±	++	±	++	±	+
0.001 μM	ND	ND	ND	ND	±	ND	±	ND	ND	ND	ND	ND	ND

ND, not determined.

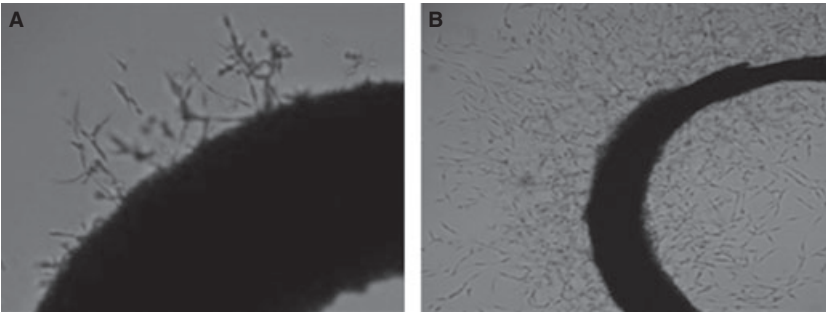


Figure 2: Identification of angiogenesis ex vivo by aortic ring sprouting assay.

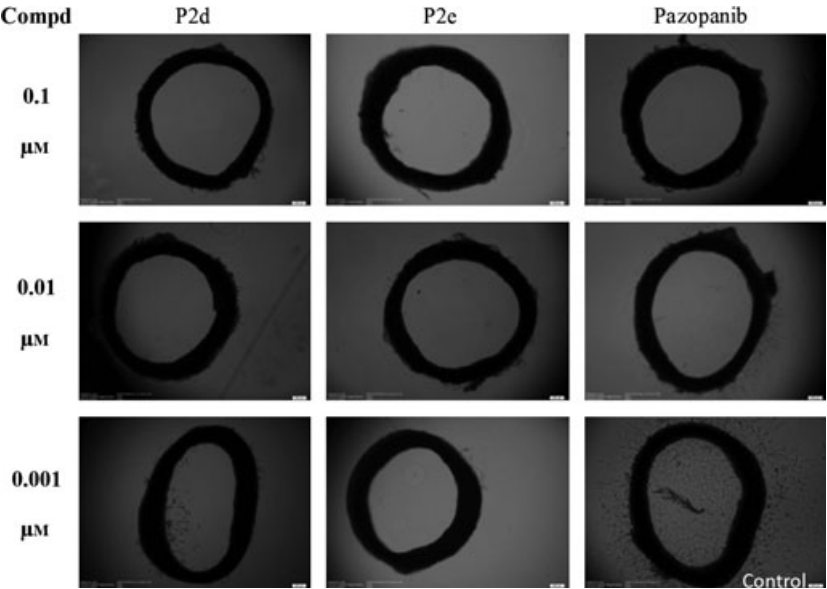


Figure 3: Compound **P2d** and **P2e** inhibit the tube formation in vitro by rat aortic ring assay.

outgrowth and inhibit the formation of tube at the concentration of $0.001\ \mu\text{M}$ (Table 4, Figure 3). All the compounds displayed a dose-dependent inhibitory activity in reducing microvascular outgrowth.

Angiogenesis involves the differentiation, proliferation and migration of endothelial cells, leading to tubulogenesis and the formation of vessels (19). Angiogenesis plays a pivotal role in the progression of solid tumors as small as 1–2 mm in diameter. The VEGF family is involved in this process (20). The ABL kinases including ABL (ABL1) and Arg (ABL2), regulate cell proliferation, survival, and stress responses (18). ABL (ABL1) is translocated next to the BCR gene [t(9;22)], generating a BCR- ABL fusion protein that has constitutively active tyrosine kinase activity (21). BCR- ABL as Activated forms of the ABL kinases can induce VEGF expression (22,23). VEGF binds to the cell surface receptors VEGFR-1, VEGFR-2, and VEGFR-3, which subsequently leads to the recruitment of ATP. ATP in turn binds to ATP-binding pocket of VEGFR, causing activation of the VEGF signaling pathway which is important for angiogenesis (22).

Compounds **P2d** and **P2e** showed both higher kinase inhibitory activity against VEGFR-2 and ABL1, and higher anti-angiogenic activity than pazopanib. One reason may be that Compounds **P2d** and **P2e** inhibit VEGFR kinase activity or molecules of signaling pathways related to VEGFR and then inhibit angiogenesis. Another reason may be that Compounds **P2d** and **P2e** inhibit the ABL1 kinase activity and then inhibit the proliferation, migration of endothelial cells and VEGF expression, and then inhibit the formation of vessels. The exact mechanism remains to be further studied.

Conclusion

In summary, we report here the synthesis and biological evaluation of a series of pazopanib derivatives as potential antitumor agents. Most compounds possess good inhibitory activities towards VEGFR-2, ABL1, and ALK1 compared with Pazopanib. Especially, compounds **P2d** and **P2e** containing the pyrimidine structure on the sulfonamide moiety demonstrated outstanding inhibitory activity against VEGFR-2 and ABL1 when compared with Pazopanib. Furthermore, the results of TARs assay showed that compounds **P2d** and **P2e** also exhibited excellent anti-angiogenic activity than that of pazopanib and even could reduce microvascular outgrowth and inhibit the formation of tube at the concentration of $0.001\ \mu\text{M}$. Overall, compounds **P2d** and **P2e**, with excellent activity both in the enzymatic inhibition assay and the anti-angiogenic assay, could be used as drug candidates for development of anticancer agents.

Acknowledgments

This work was supported by the Ph.D. Programs Foundation of Ministry of Education of P.R. China (No.

20110131110037), The Shandong Provincial Natural Science Foundation, China (Program ZR2010CQ034) and The National Natural Science Foundation of China (Grant No. 21172134). National High Technology Research and Development Program of China (Grant No. 2011ZX09401-015).

References

- Hanahan D., Folkman J. (1996) Patterns and emerging mechanisms of the angiogenic switch during tumorigenesis. *Cell*;86:353–364.
- Kerbel R.S. (2000) Tumor angiogenesis: past, present and future. *Carcinogenesis*;21:505–515.
- Chi A.S., Sorensen A.G., Jain R.K., Batchelor T.T. (2009) Angiogenesis as a therapeutic target in malignant gliomas. *Oncologist*;14:621–636.
- Dixelius J., Makinen T., Wirzenius M., Karkkainen M.J., Wernstedt C., Alitalo K., Claesson-Welsh L. (2003) Ligand-induced vascular endothelial growth factor receptor-3 (VEGFR-3) heterodimerization with VEGFR-2 in primary lymphatic endothelial cells regulates tyrosine phosphorylation sites. *J Biol Chem*;278:40973–40979.
- Olsson A.K., Dimberg A., Kreuger J., Claesson-Welsh L. (2006) VEGF receptor signalling - in control of vascular function. *Nat Rev Mol Cell Biol*;7:359–371.
- Zhong H., Bowen J.P. (2007) Molecular design and clinical development of VEGFR kinase inhibitors. *Curr Top Med Chem*;7:1379–1393.
- Xu D., Wang T.L., Sun L.P., You Q.D. (2011) Recent progress of small molecular VEGFR inhibitors as anti-cancer agents. *Mini Rev Med Chem*;11:18–31.
- Sonpavde G., Hutson T.E. (2007) Pazopanib: a novel multitargeted tyrosine kinase inhibitor. *Curr Oncol Rep*;9:115–119.
- Harris P.A., Bloor A., Cheung M., Kumar R., Crosby R.M., Davis-Ward R.G., Epperly A.H. *et al.* (2008) Discovery of 5-[[4-[(2,3-dimethyl-2H-indazol-6-yl)methylamino]-2-pyrimidinyl] amino]-2-methyl-benzenesulfonamide (Pazopanib), a novel and potent vascular endothelial growth factor receptor inhibitor. *J Med Chem*;51:4632–4640.
- Rini B. (2009) Vascular endothelial growth factor-targeted therapy in metastatic renal cell carcinoma. *Cancer*;115:2306–2312.
- Bukowski R.M., Yasothan U., Kirkpatrick P. (2010) Pazopanib. *Nat Rev Drug Discov*;9:17–18.
- Sloan B., Scheinfeld N.S. (2008) Pazopanib, a VEGF receptor tyrosine kinase inhibitor for cancer therapy. *Curr Opin Investig Drugs*;9:1324–1335.
- Limvorasak S., Poasdas E.M. (2009) Pazopanib: therapeutic developments. *Expert Opin Pharmacother*;10:3091–3102.
- Oda K., Matsuoka Y., Funahashi A., Kitano H. (2005) A comprehensive pathway map of epidermal growth factor receptor signaling. *Mol Syst Biol*;1:0010.
- Larsen A.K., Ouaret D., El Ouadrani K., Petitprez A. (2011) Targeting EGFR and VEGFR pathway

- cross-talk in tumor survival and angiogenesis. *Pharmacol Ther*;31:80–90.
16. Lamouille S., Mallet C., Feige J.J., Bailly S. (2002) Activin receptor-like kinase 1 is implicated in the maturation phase of angiogenesis. *Blood*;100:4495–4501.
 17. Swerlick R.A. (1995) Angiogenesis. *J Dermatol*; 22:845–852.
 18. Pendergast A.M. (2002) The Abl family kinases: mechanisms of regulation and signaling. *Adv Cancer Res*;85:51–100.
 19. Carmeliet P. (2005) Angiogenesis in life, disease and medicine. *Nature*;438:932–936.
 20. van Geel R.M., Beijnen J.H., Schellens J.H. (2012) Concise drug review: pazopanib and axitinib. *Oncologist*;17:1081–1089.
 21. Pendergast A.M.. (2001) BCR-ABL protein domain, function, and signaling. In: Carella A.M., Daley G.Q., Eaves C.J., Goldman J.M., Helmanns R., editors. *Chronic Myeloid Leukaemia: Biology and Treatment*. London: Martin Dunitz Ltd.; p. 19–39.
 22. Mayerhofer M., Valent P., Sperr W.R., Griffin J.D., Sillaber C. (2002) BCR/ABL induces expression of vascular endothelial growth factor and its transcriptional activator, hypoxia inducible factor-1 α , through a pathway involving phosphoinositide 3-kinase and the mammalian target of rapamycin. *Blood*;100:3767–3775.
 23. Srinivasan D., Plattner R. (2006) Activation of Abl tyrosine kinases promotes invasion of aggressive breast-cancer cells. *Cancer Res*;66:5648–5655.